Geochemical Journal, Vol. 55, pp. 171 to 183, 2021 doi:10.2343/geochemj.2.0627

Isotopic analysis of nickel, copper, and zinc in various freshwater samples for source identification

Shotaro Takano,[1]* Mao Tsuchiya,[1] Shoji Imai,[2] Yuhei Yamamoto,[2] Yusuke Fukami,[3] Katsuhiko Suzuki[3] and Yoshiki Sohrin[1]

[1]Institute for Chemical Research, Kyoto University, Japan
[2]Graduate School of Technology, Industrial, and Social Sciences, Tokushima University, Japan
[3]Japan Agency for Marine-Earth Science and Technology, Japan

(*Received January 21, 2021; Accepted April 13, 2021*)

Nickel (Ni), copper (Cu), and zinc (Zn) are commonly used in human activities and pollute aquatic environments including rivers and oceans. Recently, Ni, Cu, and Zn isotope ratios have been measured to identify their sources and cycles in environments. We precisely determined the Ni, Cu, and Zn isotope ratios in rain, snow, and rime collected from Uji City and Mt. Kajigamori in Japan, and investigated the potential of isotopic ratios as tracers of anthropogenic materials. The isotope and elemental ratios suggested that road dust is the main source of Cu in most rain, snow, and rime samples and that some of the Cu may originate from fossil fuel combustion. Zinc in the rain, snow, and rime samples may be partially attributed to Zn in road dust. Zinc isotope ratios in the Uji rain samples are lower than those in the road dust, which would be emitted via high temperature processes. Nickel isotope ratios are correlated with V/Ni ratios in the rain, snow, and rime samples, suggesting that their main source is heavy oil combustion. Furthermore, we analyzed water samples from the Uji and Tawara Rivers and the Kakita River spring in Japan. Nickel and Cu isotope ratios in the river water samples were significantly heavier than those in rain, snow, and rime samples, while Zn isotope ratios were similar. This is attributed to isotopic fractionation of Cu and Ni between particulate-dissolved phases in river water or soil.

Keywords: spring water, rain, snow, rime, river

Introduction

Heavy metals, such as Fe, Mn, Ni, Cu, Zn, and Pb are commonly used in human activities and pollute aquatic environments including rivers and oceans. The enrichment of aquatic environments with heavy metals affects aquatic organisms including phytoplankton (Morel and Price, 2003; Stefania *et al*., 2017). Anthropogenic metals emitted from industrial and residential wastewater flow into the aquatic environment. In addition, anthropogenic metal emissions in the atmosphere are transferred to the aquatic environment via dry and wet deposition. It is difficult to evaluate the amount of metals in the aquatic environment that is supplied by human activities, because of the natural sources of metals that include rock weathering, decomposition of organic matter, and input of mineral dust (Chester and Jickells, 2012).

The development of multi-collector inductively coupled plasma mass spectrometry (MC-ICP-MS) has allowed for the quick and precise measurements of isotope ratios for heavy metals. Their isotope ratios are widely used as powerful tracers of the sources of trace metals in various fields including the ocean (Cameron and Vance, 2014; Conway and John, 2014; Homoky *et al*., 2013; Vance *et al*., 2008), river (Chen *et al*., 2008), soil (Bigalke *et al*., 2010; Ratié *et al*., 2016), and atmosphere (Dong *et al*., 2013, 2017; Ochoa-Gonzalez *et al*., 2016). In particular, isotope ratios of multi-elements powerfully constrain sources and processes associated with their elements (Guinoiseau *et al*., 2018; John and Conway, 2014; Souto-Oliveira *et al*., 2019; Takano *et al*., 2020). For example, Souto-Oliveira *et al*. (2018, 2019) have determined Cu, Zn, and Pb isotope ratios in atmospheric particles collected in Sao Paulo, and determined the sources of these metals, such as vehicular traffic, construction activities, and metallurgical industries.

The multi-elemental isotopic study of heavy metals for atmospheric wet deposition has not been conducted previously. Wet deposition is a dominant mechanism for transporting atmospheric particles to the Earth's surface in East Asia. In southeast China, wet deposition fluxes of Cu and Zn are 1.5–6 times more than the dry depositions (Ye *et al*., 2018). In this study, we present an effective and precise method for determining Ni, Cu, and Zn isotope ratios in freshwater samples. This method can simultaneously separate Ni, Cu, and Zn from freshwater

*Corresponding author (e-mail: takano.shotaro.3r@kyoto-u.ac.jp)

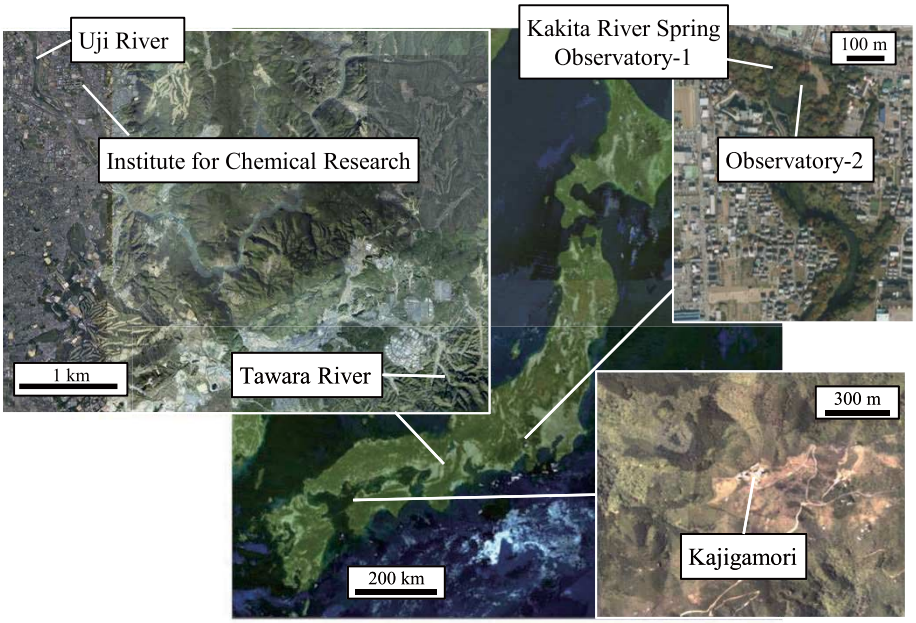

Fig. 1. Sampling sites. River water was collected from the Uji and Tawara Rivers. Rainwater was collected at the Institute for Chemical Research and Mt. Kajigamori. Spring water was collected from Observatory-1 and Observatory-2 in the Kakita River spring. This figure is based on the Digital Basic Map published by the Geospatial Information Authority of Japan.

samples only using two-step separation, and successfully determine their isotope ratios using a MC-ICP-MS. Then, we analyze the Ni, Cu, and Zn isotope ratios in rainwater, snow, rime, spring, and river water collected in Japan to evaluate the potential of the isotope ratios of metals as tracers of anthropogenic materials in aquatic environments.

METHOD

Reagents and materials

Ultrapure water was supplied by Milli-Q integral MT or Milli-Q IQ 7005 water purification system (Millipore). High purity reagents of HCl, HNO_3, HF (Ultrapur-100, Kanto Chemical), H_2O_2 (Tamapure-AA10, Tama Chemicals) and CH_3COOH (Optima, Fisher Scientific) were used for sample preparation. Standard solutions for elemental concentration measurements were prepared by mixing commercial standard solutions (Na, Mg, Al, Ca, Ti, V, Cr, Mn, Fe, Ni, Cu, Zn, Ga, Mo, Cd, Ba, and Pb; Wako Pure Chemical Industries). For isotopic measurements, secondary standard materials (Ni_{Wako}, Cu_{Wako}, and $Zn_{AA\text{-}ETH}$) certified by primary reference materials ($Ni_{NIST\ SRM986}$, $Cu_{NIST\ SRM976}$, and $Zn_{JMC\text{-}Lyon}$) were used (Archer *et al*., 2017; Takano *et al*., 2017).

Polytetrafluroacetate (PFA) vials (Savillex) were cleaned by soaking in diluted alkaline detergent for 12 h, rinsed with ultrapure water, and then boiled in 3 M HNO_3 for 2 h before rinsing with ultrapure water. Disposable lab wares, such as pipette tips and centrifuge tubes, were soaked in warm 3 M HNO_3 and rinsed with ultrapure water.

Samples

Sampling sites are shown in Fig. 1. Rainwater samples were collected from the rooftop of the Institute for Chemical Research, Kyoto University, Uji, Kyoto (34.910°N, 135.802°E). Uji is a suburban city with 180,000 habitants. Rainwater, snow, and rime samples were collected from the top of Mt. Kajigamori, Otoyo, Kochi (33.759°N, 133.752°E) in the Shikoku Mountains. Spring water samples that originate from Mt. Fuji were collected at observatory-1 (35.108°N, 138.900°E) and observatory-2 (35.107°N, 138.901°E) at Kakita River Park, Shimizu, Shizuoka. River water samples were collected from the Uji River, Uji, Kyoto (34.917°N, 135.790°E) and the Tawara River, Ujitawara, Kyoto (34.846°N, 135.899°E), which is a tributary flowing into the Uji River. Rainwater samples were collected in low-density polyethylene (LDPE) bottles attached to a polyethylene (PE) funnel (Yamamoto *et al*., 2019). Snow samples were collected in plastic containers and transferred to LDPE bottles. Rime samples were collected from those grown on a PE net. River water samples were collected using a PE bucket and a PE rope. Spring water samples were collected using a polytetrafluoroethylene (PTFE) beaker or PTFE Bailer sampler with a Kevlar rope. Samples were filtered using 0.45 μm membrane filters

(Millex, Millipore) and the filtrates were acidified to 0.02 M HNO_3. In addition, riverine standard material SLRS-5 (National Research Council of Canada) was used to validate our analysis.

To assess the contribution of mineral dust to fresh water, a leaching experiment of sand was carried out: metals were leached from 238 mg of a sand sample collected from Luntai in the northern Taklamakan Desert (site 79, Chang *et al*., 2000) with 500 g of ultrapure water for 90 h at room temperature, and the obtained supernatant was acidified using 0.02 M HNO_3.

Solid-phase chelate extraction

Nickel, Cu, and Zn were preconcentrated from samples by solid-phase chelate extraction. The chelate extraction process was based on previous studies (Takano *et al*., 2017, 2020) and was performed inside a clean booth. A NOBIAS Chelate PA-1W column (Hitachi high technologies) was used for chelate extraction. The column made of polypropylene contained 600 mg of NOBIAS Chelate PA-1 resin. Before preconcentration, a sample with a CH_3COOH-CH_3COONH_4 buffer (final concentration 0.03 M) was added to adjust the pH to 4.6–5.0. All solutions except for the eluent were passed through the column by a peristaltic pump. A sample solution was passed through the column at a flow rate of 10 mL/min (Supplementary Table S1) after cleaning and conditioning the inside of the column. Subsequently, ultrapure water was passed at 60 mL/min to remove alkali metals and earth metals. Then, 1.5 M NH_4F (pH 3.8–4.0) solution was passed at 1 mL/min to elute Al, Ti, Fe, V, and Mn from the resin after which, ultrapure water was passed at 60 mL/min. Finally, 8 mL of 1 M HNO_3 was passed through the column by gravity to elute metals absorbed on the resin. The eluate was completely evaporated on a hot plate (180°C) and the residue was dissolved in 0.4 mL of 15 M CH_3COOH-1.7 M HCl.

Anion exchange separation

Samples preconcentrated by chelate extraction were processed by anion exchange to separate Ni, Cu, and Zn from matrices. Supplementary Table S2 shows the procedure of anion exchange. The anion exchange column was made of PFA tubing and a polyethylene frit. The dimensions were 1 cm bed height by a 3 mm inner diameter. AG MP-1M anion exchange resin (100–200 mesh, Bio-Rad) was packed into the column. Samples and eluents were added to the column using a pipette and passed by gravity. Before loading the samples, the resin was cleaned with 1.5 mL of 1 M HNO_3 and conditioned with 0.4 mL of 15 M CH_3COOH-1.7 M HCl. Then, a sample dissolved in 0.4 mL of 15 M CH_3COOH-1.7 M HCl, and 0.3 mL of 15 M CH_3COOH-1.7 M HCl was subsequently passed through the anion exchange column to collect Ni. To elute Ti and Mn, 1 mL of 12 M CH_3COOH-1.7 M HCl and 0.1 mL of 10 M HCl were passed, respectively. Copper was eluted with 2.5 mL of 4 M HCl. After the elution of Fe and Mo with 1 mL of 1 M HCl, Zn was eluted with 1 mL of 1 M HNO_3. The eluates of Ni, Cu, and Zn were evaporated, and the organic residue was digested by reflux in 1 mL of 69% HNO_3 and 0.1 mL of 35% H_2O_2 for 12 h at 160°C on a hotplate. After evaporation of the acid, the Ni fraction was dissolved in 2% HNO_3 and the Cu and Zn fractions in 0.3% HNO_3.

Measurements of isotope ratios

Nickel, Cu, and Zn isotope measurements were performed on a Neptune Plus MC-ICP-MS (Thermo Fisher Scientific) at the Research Institute for Humanity and Nature and on a different Neptune Plus at the Japan Agency for Marine-Earth Science and Technology. The cup configurations are shown in Supplementary Table S3. Sample and standard solutions were introduced to the MC-ICP-MS via a PFA nebulizer (50 μL/min flow rate) and a glass spray chamber for Cu isotope measurements, and via a PFA nebulizer and an Aridus II desolvater (Cetac) for Ni and Zn isotope measurements. With respect to Ni measurements, N_2 gas was added to sweep gas of Aridus II at a flow rate of 5 mL/min to decrease interferences of oxides, such as $^{40}Ar^{18}O^+$ and $^{42}Ca^{16}O^+$. Copper was measured at a low-resolution mode, and Ni and Zn were measured at a high-resolution mode. Data collection consisted of 4.2 s × 20–30 cycles.

Interferences of isobar ions or double charged ions were corrected using Eq. (S1) in Supplementary material. The Fe interference on Ni was corrected by measuring $^{58}Fe^+$, the Ba^{2+} interferences on Cu, Ga, and Zn were corrected by measuring $^{137}Ba^{2+}$, and the Ni interference on Zn was corrected by measuring $^{62}Ni^+$.

Mass biases in Ni and Zn isotope measurements were corrected using the double-spike technique. The detailed calculation and procedure were described in previous studies (Siebert *et al*., 2001; Takano *et al*., 2017). Double spikes of ^{61}Ni-^{62}Ni and ^{64}Zn-^{67}Zn were added to samples more than 12 h before chemical separation. δ^{60}Ni and δ^{66}Zn were calculated relative to secondary standards (i.e., Ni_{Wako} and $Zn_{AA\text{-}ETH}$). For Cu isotope measurements, mass biases were corrected by standard-bracketing in combination with the external correction method using Ga isotopes. After chemical separation, a Ga standard solution (Ga_{Wako}, Wako Pure Chemicals) was added to be 1000 ppb in sample solution. A standard solution containing 400 ppb of Cu_{Wako} and 1000 ppb of Ga_{Wako} was measured every 2–4 samples. δ^{65}Cu was calculated relative to Cu_{Wako} via the method described in previous studies (Maréchal *et al*., 1999; Takano *et al*., 2013). Measured δ values of Ni, Cu, and Zn relative to Ni_{Wako}, Cu_{Wako}, and $Zn_{AA\text{-}ETH}$ were expressed as $\delta^{60}Ni_{Wako}$, $\delta^{65}Cu_{Wako}$, and

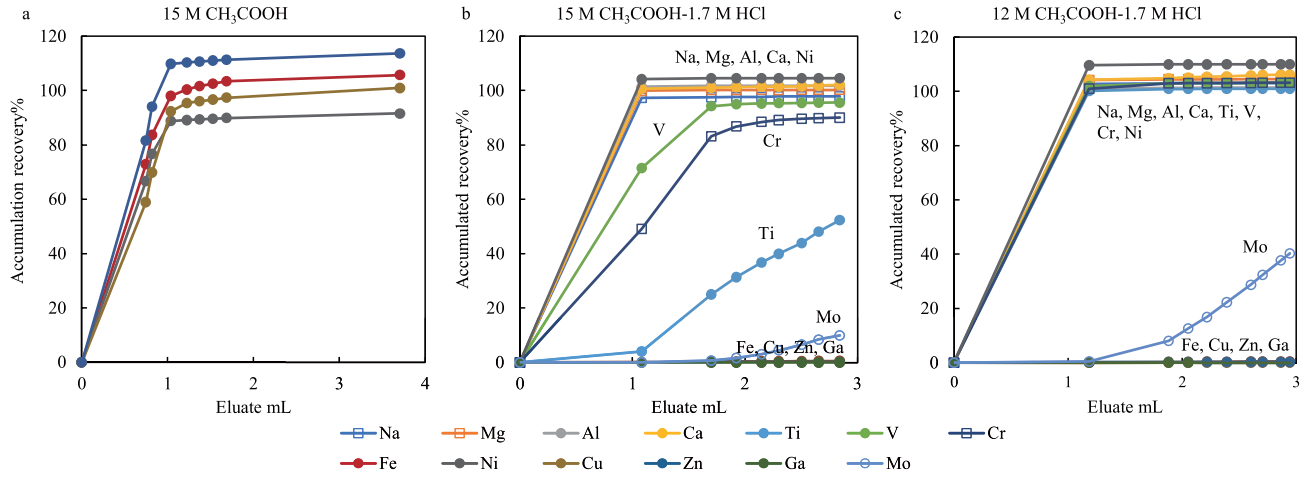

Fig. 2. Elution curves of anion exchange for metal ions using 15 M CH_3COOH (a), 15 M CH_3COOH-1.7 M HCl (b), or 12 M CH_3COOH-1.7 M HCl (c).

$\delta^{66}Zn_{AA\text{-}ETH}$, and those relative to primary standards as $\delta^{60}Ni_{NIST986}$, $\delta^{65}Cu_{NIST976}$, and $\delta^{66}Zn_{JMC\text{-}Lyon}$, respectively. $\delta^{60}Ni_{NIST986}$, $\delta^{65}Cu_{NIST976}$, and $\delta^{66}Zn_{JMC\text{-}Lyon}$ were calculated by subtracting the δ value of the secondary standard (Archer *et al.*, 2017; Takano *et al.*, 2017).

Measurements of elemental concentrations

Concentrations of Ni and Zn were determined using the isotope dilution method at the same time as the isotopic measurement. The concentration of Cu was measured by comparison of the ^{63}Cu signal intensity with the bracketing standards in the isotopic measurement. Concentrations of the other elements in rain, rime, river, and spring water samples were determined by the calibration curve method using an Element 2 HR-ICP-MS (Thermo Fisher Scientific) at the Institute for Chemical Research, Kyoto University.

Results and Discussion

Recoveries and procedural blanks in chemical separation

Some freshwater samples contain large amounts of Al, Mn, V, and Fe, all of which cause potential interferences during isotope measurements of Ni, Cu, and Zn. Aluminum, Mn, and Fe are effectively removed by passing an NH_4F solution through the NOBIAS Chelate-PA1 column after sample loading (Takano *et al.*, 2020). We evaluated the removal efficiency of interfering elements in chelating extraction using solutions of different pH of NH_4F. After conditioning, 1 L ultrapure water with 2 μg of Na, Mg, Al, Ca, Ti, V, Cr, Mn, Fe, Co, Ni, Cu, Zn, Ga, Mo, Cd, and Ba was passed through the NOBIAS Chelate-PA1 column, and subsequently an NH_4F solution with a pH ranging from 3.8–4.0 or that with a pH ranging from 4.6–4.9. Furthermore, 1 M HNO_3 was passed for elution. Metal recoveries were determined via the measurement of the eluate (Supplementary Fig. S1). The NH_4F solution with a pH of 3.8–4.0 was more effective in removing Al, Mn, V, Fe, Ga, and Mo. The recoveries of Ni, Cu, and Zn through the optimal procedure of chelate extraction (Table S1) are 96.2 ± 1.9%, 95.9 ± 1.3%, and 96.6 ± 1.2% (mean ± 1 standard deviation, SD), respectively.

Generally, Cu is isolated by anion exchange using HCl media (Borrok *et al.*, 2007; Maréchal *et al.*, 1999; Yamakawa *et al.*, 2009). However, because the distribution coefficient of Cu on the anion exchange resin is low, an anion exchange column with a long bed height or multiple cycles of ion exchange is required to separate Cu from the other metals, such as Ti and Na. Recently, it has been reported that Cu is successfully separated via an anion exchange column with a short bed height using a CH_3COOH-HCl media (Yang *et al.*, 2019). We optimized CH_3COOH and HCl concentrations in the media used for anion exchange. First, 15 M CH_3COOH (0.85 mL) containing 250 ng each of Fe, Ni, Cu, and Zn was passed through an anion exchange resin column of 5 cm bed height. However, all the metals were not adsorbed on the anion exchange resin in 15 M CH_3COOH (Fig. 2a). It is suggested that metal complexes in pure CH_3COOH are cations or neutral species. According to the results of molecular structure analysis using the electron spin resonance spectrum (Sharrock and Melník, 1985), Cu is present as a neutral complex $[Cu(CH_3COO)_2{\cdot}(H_2O){\cdot}CH_3COOH]$ in CH_3COOH solution.

Next, 15 M CH_3COOH-1.7 M HCl or 12 M CH_3COOH-1.7 M HCl were used as media in anion exchange. The CH_3COOH-HCl solution (0.85 mL) contain-

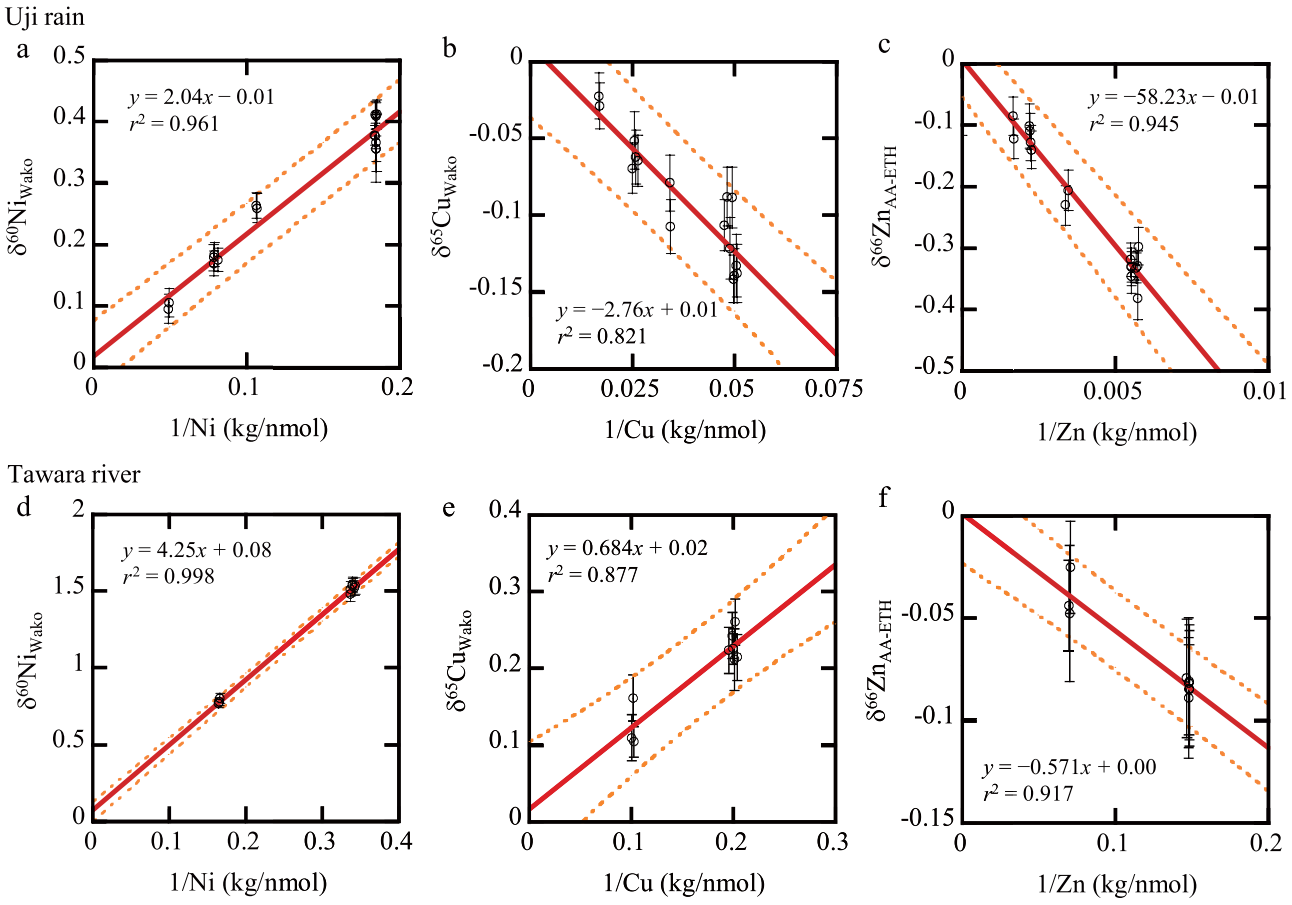

Fig. 3. Isotope ratios plotted against the reciprocal concentrations for Ni (a, d), Cu (b, e), and Zn (c, f) in Uji rainwater (a, b, c) and the Tawara River water (d, e, f) with/without doping the secondary standards of Ni, Cu, and Zn. Error bars indicate 2-standard error of δ values in MC-ICP-MS measurements. The linear regression curves are shown as solid lines. The 95% prediction bands are shown as dashed lines.

ing 2900 ng Na, 710 ng Mg, 1100 ng Al, 700 ng Ca, 760 ng Ti, 730 ng V, 720 ng Cr, 770 ng Fe, 710 ng Ni, 790 ng Cu, 690 ng Zn, 90 ng Ga, and 1400 ng Mo was passed through an anion exchange column of 1 cm bed height. After that, the same CH_3COOH-HCl solution without metals was passed to elute metals from the anion exchange column (Figs. 2b and 2c). In CH_3COOH-HCl solutions, Cu was adsorbed on the anion exchange resin, suggesting that Cu was present as an anion complex $[Cu(CH_3COO)_2 \cdot Cl \cdot CH_3COOH]^-$ by replacing a water molecule in $[Cu(CH_3COO)_2 \cdot (H_2O) \cdot CH_3COOH]$ with a Cl^- ion. In 15 M CH_3COOH-1.7 M HCl, the anion exchange resin column retained ~100% of Ti, Fe, Cu, Zn, Ga, Mo, and 71% of V after passing 1 mL of eluent. In 12 M CH_3COOH-1.7 M HCl, Ti, V, and Cr were more rapidly eluted. Therefore, we decided to use 15 M CH_3COOH-1.7 M HCl for elution of Ni, and 12 M CH_3COOH-1.7 M HCl for elution of Ti, V, and Cr. For the elution of Fe, Cu, and Zn, we used 1 M HCl, 4 M HCl, and 1 M HNO_3, respectively (Table S2).

The recoveries of 15 elements through anion exchange using columns of 1 cm bed height are shown in Supplementary Table S4. Nickel is eluted concurrently with alkali metals and alkali earth metals. However, most of these metals are removed by chelate extraction prior to anion exchange. Although 60% of the Mn is eluted together with Cu in anion exchange, more than 99.9% of the Mn is also removed in chelate extraction. In the previous study (Takano *et al.*, 2017), the anion exchange process using a long column of 7 cm took 10–11 h. In this study, the short bed height of the column reduced the processing time to 5–6 h.

We evaluated procedure blanks through this analytical method, by processing 1 L of ultrapure water as a sample. The procedure blanks of Ni, Cu, and Zn were 0.007 ± 0.002 nmol, 0.007 ± 0.004 nmol, and 0.02 ± 0.01 nmol (n = 8), respectively. The minimum amounts of Ni, Cu, and Zn contained in our natural water samples were 0.245

Table 1. Isotope ratios and concentrations of Ni, Cu, and Zn in a certified material of river water SLRS-5

		$\delta^{60}Ni_{NIST986}$		$\delta^{65}Cu_{NIST976}$		$\delta^{66}Zn_{JMC\text{-}Lyon}$		Concentration nmol/kg		
		Mean	2SE[a]	Mean	2SE[a]	Mean	2SE[a]	Ni	Cu	Zn
SLRS-5	#1	0.69	0.05	0.50	0.02	0.38	0.02	7.92	289	13.2
	#2	0.75	0.05	0.49	0.02	0.39	0.03	7.95	288	13.2
	#3	0.72	0.05	0.50	0.02	0.36	0.02	8.08	295	13.2
	Mean	0.72		0.50		0.38		7.98	291	13.2
	2SD[b]	0.05		0.02		0.03		0.17	7	0.02
Certified value								8.11 ± 1.09	274 ± 20	12.9 ± 1.5

[a]*2-standard error in MC-ICP-MS measurements.*
[b]*2-standard deviation in replicate analyses.*

nmol, 0.259 nmol, and 2.00 nmol, respectively. The contributions of the procedure blanks were less than 3% for Ni, 3% for Cu, and 1% for Zn.

External correction using Ga in the isotope measurement of Cu

The instrumental mass bias during Cu isotope measurements is often corrected by external correction using Zn isotopes. This correction is sensitive to the Zn/Cu ratio in measured solutions. Different Zn/Cu ratios between the sample and the standard solution cause an analytical artifact (Archer and Vance, 2004; Zhu *et al*., 2015). Therefore, Zn must be doped to achieve a constant Zn/Cu ratio among the samples and the standard solution for accurate isotope measurement. Instead of Zn, Ga is used for the external correction of the Cu isotope measurement in this study. Figure S2 shows $\delta^{65}Cu_{Wako}$ values measured in 100 ppb Cu_{Wako} solution doped with different amounts of Ga_{Wako} or $Zn_{AA\text{-}ETH}$. Only when the Zn/Cu ratio is identical to the standard solution (Zn/Cu = 3), $\delta^{65}Cu_{Wako}$ is ~0. δ^{65}Cu values shift to the positive direction for solutions containing higher Zn/Cu ratios, and vice versa. The shift in δ^{65}Cu is attributable to the interference of $^{64}Zn^{1}H$ on ^{65}Cu. In the case of Ga doping, $\delta^{65}Cu_{Wako}$ is ~0 at any Ga/Cu ratios, and matching Ga/Cu ratios between the sample and standard solutions are not required. Therefore, the use of Ga for external correction allows for more accurate and simpler measurements of Cu isotopes.

Interferences during isotope measurements of Ni, Cu, and Zn

Various ions cause interferences during the isotope measurements of Ni, Cu, and Zn. In Supplementary Fig. S3 and Supplementary Table S5, we evaluated the interferences of Na, Mg, Ti, Cr, Mn, and Ba in measurements for Cu isotopes; Ca, Ti, and Fe in measurements for Ni isotopes, and Mg, Al, Ca, Ti, V, Cr, and Ba in measurements for Zn isotopes (Table S5). Isotope ratios of Ni_{Wako}, Cu_{Wako}, and $Zn_{AA\text{-}ETH}$ were measured after doping with these interfering elements. In measurements of Ni isotopes, a detectable interference (>0.05‰) was not caused by Fe. The interference was sufficiently corrected using the intensity of ^{57}Fe (Eq. S1). Interferences of Ca and Ti were not observed below 29 mol/mol of Ca/Ni and 0.45 mol/mol of Ti/Ni, respectively. For measurements of δ^{65}Cu, the shifts exceeding 0.05‰ were caused by interferences of Ti and Mn at >0.04 mol/mol Ti/Cu and >0.5 mol/mol Mn/Ga, respectively. The interference of Cr was not observed below 0.05 mol/mol of Cr/Cu, and that of Ba was successfully corrected by $^{137}Ba^{2+}$ intensity. For measurements of Zn isotopes, detectable interferences were not found in our experiment. Supplementary Figure S4 shows ratios of potentially interfering elements to Ni, Cu, or Zn in natural water samples (i.e., snow, rime, river water, and rain) after chemical separation. Threshold lines in Fig. S4 indicate maximum elemental ratios below which undetectable interference is observed. For most of the samples, the elemental ratios are below these lines, thus indicating the effectiveness of our method in removing interfering elements for isotopic measurements of Ni, Cu, and Zn. The samples containing interfering elements above the threshold lines are excluded from the following sections.

Accuracy and precision

The accuracy and precision of the isotope analyses of Ni, Cu, and Zn were evaluated by repeat analysis of river water collected from the Tawara River on October 10, 2019 and rainwater collected from Uji City from July 23 to 27, 2019. The river water was divided into nine subsamples of 500 mL each. Three of them were doped with 1.5–1.6 nmol of Ni_{Wako}, 2.5 nmol of Cu_{Wako}, and 3.6–3.7 nmol of $Zn_{AA\text{-}ETH}$. The rainwater was divided into 16 subsamples of 500 mL each. Ten of them were doped with 1.9–7.3 nmol of Ni_{Wako}, 4.8–19.3 nmol of Cu_{Wako}, and 53–210 nmol of $Zn_{AA\text{-}ETH}$. Analyzed isotope ratios of Ni, Cu, and Zn in all the subsamples are shown in Supplementary Table S6. Recoveries of Ni, Cu, and Zn calculated using Eq. (S2) are close to 100%; 108 ± 5% for Ni, 99 ± 4% for Cu, and 92 ± 5% for Zn (mean ± SD, n = 3) for the Tawara River water and 99 ± 6% for Ni, 99 ± 4% for Cu, and 100 ± 11% for Zn (n = 8) for the rainwater.

The 2SDs for the δ values in undoped samples are <0.05‰, and we adopted the 2SDs as external uncertainties of this method. In Fig. 3, the δ values are plotted against the reciprocal concentrations for Ni, Cu, and Zn. High linearities are observed in these data, and intercepts of the regression lines are ~0, which follows a theoretical equation representing isotope ratios of binary mixtures (Eq. (S3)). This suggests that our method can accurately determine Ni, Cu, and Zn isotope ratios.

The reference material for river water (SLRS-5) was analyzed (Table 1). The concentrations were within the certified values. Although the isotope ratios of Ni, Cu, and Zn in SLRS-5 have not been reported previously, our results are within the range of reported values for river water in the world (0.78 ± 0.30‰ for δ^{60}Ni, 0.61 ± 0.29‰ for δ^{65}Cu, and 0.39 ± 0.17‰ for δ^{66}Zn) (Cameron and Vance, 2014; Little *et al*., 2014; Vance *et al*., 2008).

Metal concentrations and isotope ratios of Ni, Cu, and Zn in natural water samples

Metal concentrations (Na, Mg, Ca, Ti, V, Cr, Mn, Fe, Ni, Cu, Zn, Ga, Mo, Cd, Sb, Ba, and Pb) and isotope ratios ($\delta^{60}Ni_{NIST986}$, $\delta^{65}Cu_{NIST976}$, and $\delta^{66}Zn_{JMC\text{-}Lyon}$) in rainwater, snow, rime, river water, and spring water are compiled in Supplementary Table S7. The volume-weighted mean concentrations of metals in rainwater are compared with literature data in Table 2. The metal concentrations in this study are generally lower than literature values. This may be because most of our rainwater samples are collected between summer and fall. The northwest monsoon transports pollutants and mineral dust to Japan from the Asian continent in winter–spring, and the concentration in atmospheric particles is high in winter–spring and low in summer–fall in Japan (Pan *et al*., 2016). Considering rainwater scavenges atmospheric particles, metal concentrations in rainwater would be lower in summer–fall. Actually, metal concentrations in rainwater collected along the Japan Sea coast in winter–spring are higher than those collected in summer–fall (Sakata and Asakura, 2009).

Enrichment factors (*EFs*) relative to the continental crust are calculated as follows.

$$EF(\mathrm{X}) = \frac{\left(\frac{\mathrm{X}}{\mathrm{Al}}\right)_{\mathrm{sample}}}{\left(\frac{\mathrm{X}}{\mathrm{Al}}\right)_{\mathrm{continental\ crust}}}, \qquad (1)$$

where $(X/Al)_{sample}$ and $(X/Al)_{continental\ crust}$ are molar ratios of an element X to Al in a sample and the continental crust (Chester and Jickells, 2012), respectively. Aluminum is used as a tracer of terrigenous material. The *EFs* for all measured elements are shown in Supplementary Table S8.

Table 2. Volume-weighted mean concentrations in rainwater samples[c]

	Na[a]	Mg[a]	Al[b]	Ca[a]	Ti[b]	V[b]	Cr[b]	Mn[b]	Fe[b]	Ni[b]	Cu[b]	Zn[b]	Ga[b]	Mo[b]	Cd[b]	Sb[b]	Ba[b]	Pb[b]	Ref.
Kajigamori (Japan)	28	3.2	36	1.1	0.33	1.3	0.22	4.9	17	1.1	2.0	252	0.045	0.09	0.17	0.28	3.8	0.87	This study
Uji (Japan)	18	0.51	96	1.9	2.3	4.1	0.44	18	43	2.6	10	82	0.015	0.73	0.19	0.13	17	1.9	This study
Noshiro (Japan)	NA	NA	NA	NA	NA	8.8	4.6	84	NA	8.5	22	NA	NA	NA	1.5	1.1	NA	25	Sakata and Asakura (2009)
Nakanoto (Japan)	NA	NA	NA	NA	NA	7.1	3.5	58	NA	11	13	184	NA	NA	1.2	1.1	NA	22	Sakata and Asakura (2009)
Matsuura (Japan)	NA	NA	NA	NA	NA	7.1	3.7	55	NA	8.5	11	168	NA	NA	1.3	1.0	NA	15	Sakata and Asakura (2009)
Tsukuba (Japan)	NA	NA	1260	NA	NA	NA	NA	200	NA	NA	39	275	NA	NA	NA	3.3	NA	NA	Hou *et al.* (2005)
Higashi-Hiroshima (Japan)	6.7	1.1	225	2.4	NA	4.5	NA	30	NA	4.4	9.8	73	NA	NA	0.56	NA	2.7	6.0	Takeda *et al.* (2000)
Nam Co (China)	NA	NA	467	NA	NA	0.6	5.1	10	206	3.8	8.5	93	NA	NA	0.04	NA			Cong *et al.* (2010)
Chuncheon (Korea)	NA	NA	513	NA	NA	2.7	NA	59	NA	8.9	27	151	NA	NA	0.62	NA	13	7.3	Kim *et al.* (2012)
Clear water bay (Hong-Kong)	12	1.8	888	NA	12	13	NA	23	479	NA	29	195	NA	NA	NA	4.9	22	306	Zheng *et al.* (2005)
Kowloon (Hong-Kong)	32	3.9	474	7.7	NA	3.5	NA	27	306	NA	NA	NA	NA	NA	1.2	NA	NA	12	Tanner and Wong (2000)
South Singapore	NA	NA	683	NA	24	69	NA	51	428	65.8	88	111	NA	NA	2.9	NA	NA	16	Hu and Balasubramanian (2003)

[a]*μmol/kg*, [b]*nmol/kg*, [c]*not analyzed.*

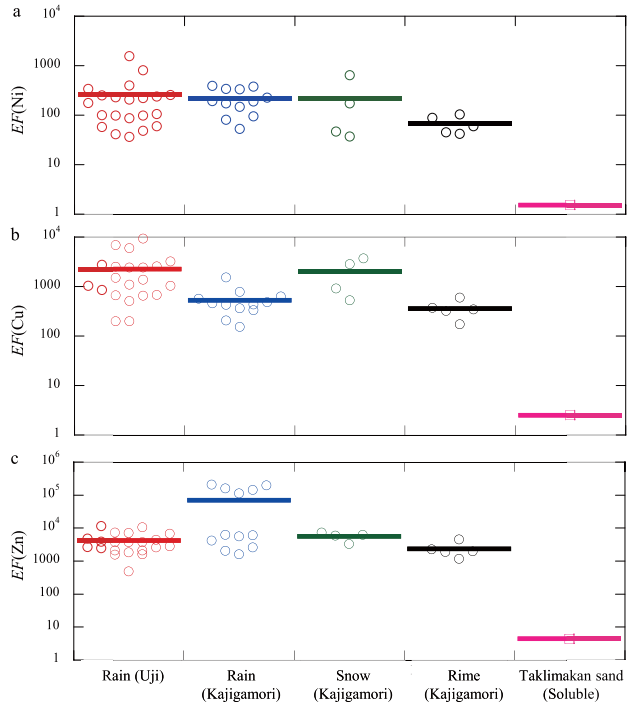

Fig. 4. Enrichment factors relative to the continental crust for Ni, Cu, and Zn in rainwater, snow, rime, and water-soluble fraction of the Taklamakan sand. Solid lines represent the mean values.

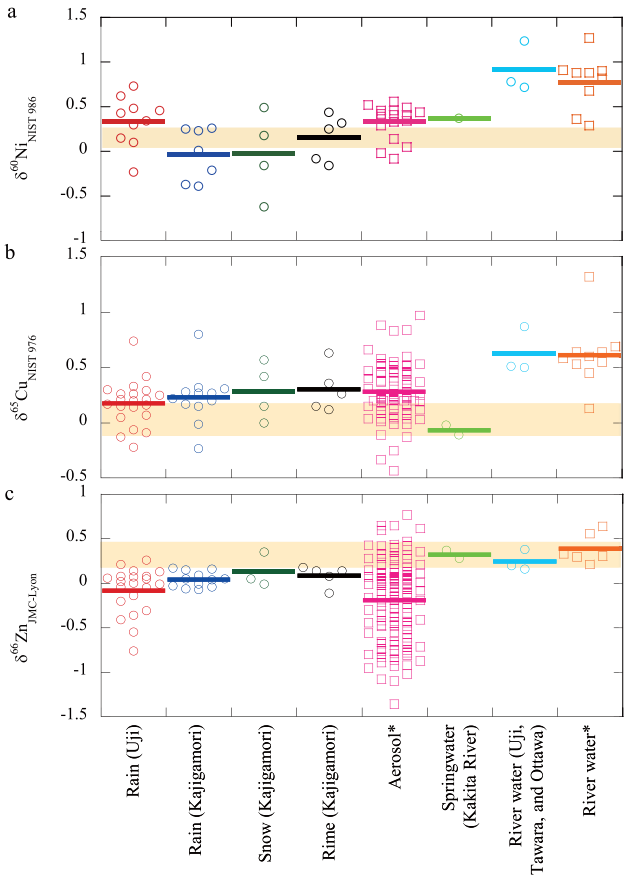

*Fig. 5. Isotope ratios of Ni, Cu, and Zn in freshwater samples and aerosols. Solid lines indicate the mean value. Yellow bands represent the mean ± 1 standard deviation in terrigenous materials (Cameron et al., 2009; Little et al., 2014). *literature data for aerosols (Dong et al., 2017; Ochoa-Gonzalez et al., 2016; Souto-Oliveira et al., 2018) and rivers (Cameron and Vance, 2014; Little et al., 2014; Vance et al., 2008).*

The *EFs* for Ni, Cu, and Zn in rain, snow, and rime samples are 10^1–10^5 (Fig. 4). One possibility to explain such high *EFs* is the different solubilities of the metals in mineral dust originated from the continental crust. However, the *EFs* in a water-soluble fraction of the Taklamakan sand is as low as 2–5, which indicates that preferential dissolution of Ni, Cu, and Zn from the mineral dust is not enough to explain the high *EFs* of the metals in rain, snow, and rime. It is to be noted that the leaching condition of mineral dust in our experiment is different from that in actual rainwater. Actual rainwater is acidic more than ultrapure water, and mineral dust in the atmosphere is finer than bulk sand. Therefore, solubilities of metals in mineral dust would be higher in actual rainwater, which may increase the *EFs* of Ni, Cu, and Zn. Another possibility explaining high *EFs* is the input of anthropogenic Ni, Cu, and Zn, as these metals are common in human activities. Correlation coefficients among metal concentrations in rain, snow, and rime are shown in Supplementary Tables S9–S12. Strong correlations are found among Al, Ti, Cr, Mn, and Fe in rain, snow, and rime samples. *EFs* of these elements are less than 100. Therefore, the dominant source of these elements would be mineral dust. Strong correlations are also observed between Na and Mg, suggesting that both these elements originate from sea salt. Correlation coefficients for V, Ni, Cu, Zn, Ba, Cd, and Pb largely vary according to location and sample types (i.e., rain, snow, and rime). These metals have high *EFs* (>100), and their anthropogenic input is significant. The high variability of the correlation coefficients suggests that these metals are from multiple sources and that the contribution of the sources varies according to location and sample types.

Isotope ratios of Ni, Cu, and Zn in rain, snow, rime, river water, and spring water samples are shown in Fig. 5, together with literature data. The isotope ratios of Cu and Zn in rainwater, snow, and rime samples are within the ranges of those of aerosols from an island in the South China Sea (Takano *et al.*, 2020), and from cities in Europe (Dong *et al.*, 2017; Ochoa-Gonzalez *et al.*, 2016) and South America (Souto-Oliveira *et al.*, 2018, 2019). Nickel isotope ratios in aerosols have been reported only

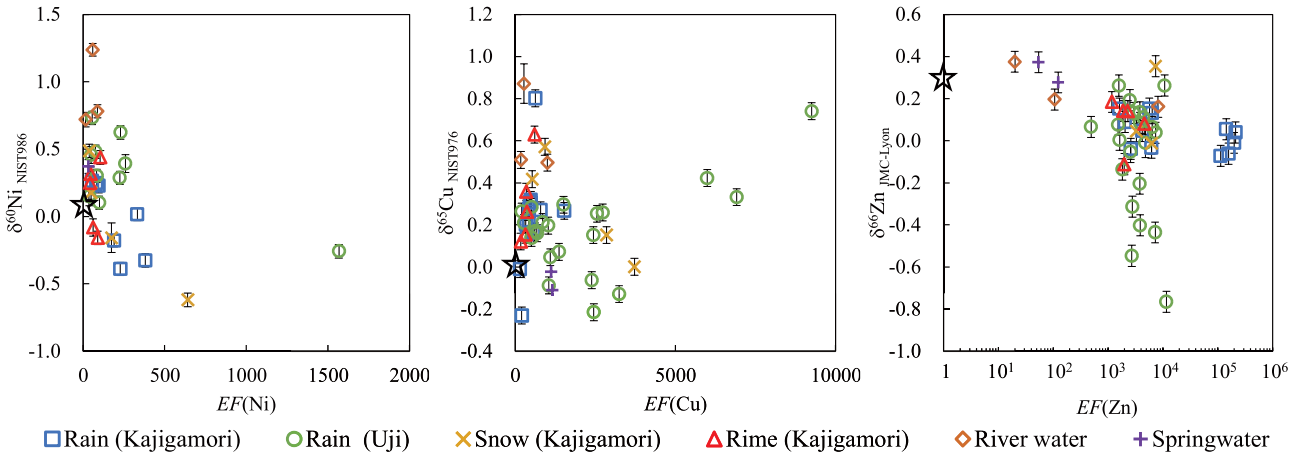

Fig. 6. Isotope ratios of Ni, Cu, and Zn in our freshwater samples plotted against enrichment factors (EF). Error bars indicate 2-standard errors of δ values in MC-ICP-MS measurements. Stars represent the mean for terrigenous materials (Cameron et al., 2009; Little et al., 2014)

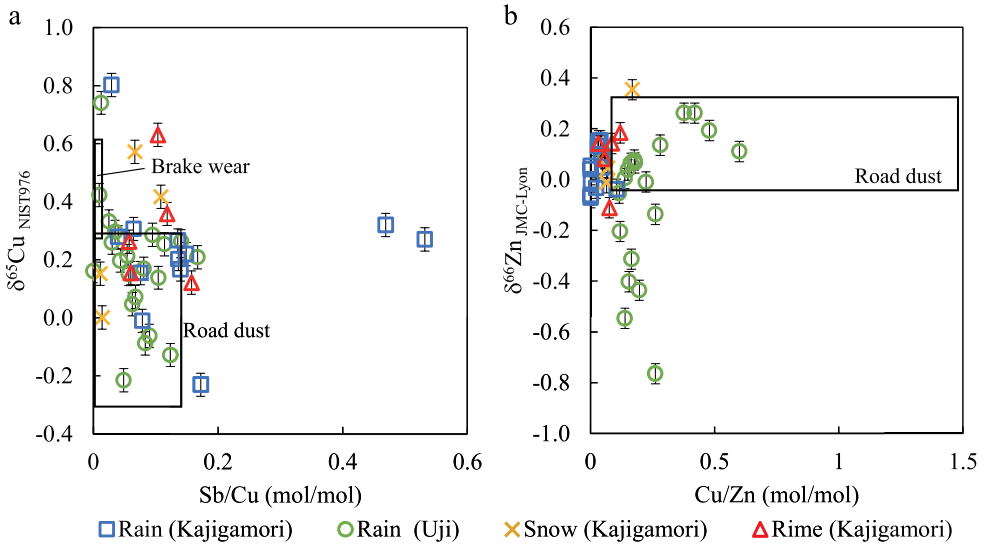

Fig. 7. $\delta^{65}Cu_{NIST976}$ values plotted against Sb/Cu ratios in rain, snow, and rime (a). Error bars indicate 2-standard errors of δ values in MC-ICP-MS measurements. $\delta^{66}Zn_{JMC\text{-}Lyon}$ values plotted against Cu/Zn ratios in rainwater, snow, and rime (b). Solid boxes represent the range of road dust (Dong et al., 2017).

for those collected from an island in the South China Sea. Variations of $\delta^{60}Ni_{NIST986}$ in rainwater, snow, and rime samples are larger than those in aerosols in the South China Sea. For rain, snow, and rime samples, Ni, Cu, and Zn isotope ratios are plotted against their *EFs* in Fig. 6. For Ni, isotope ratios are higher at lower *EFs*. For Cu, isotope ratios tend to be higher at higher *EFs* in rainwater and rime. For Zn, most of the data are plotted within the range of 10^3 to 10^4 of *EFs* and –0.1 to +0.3‰ of $\delta^{66}Zn_{JMC\text{-}Lyon}$. Several rainwater samples from Uji exhibit lower $\delta^{66}Zn_{JMC\text{-}Lyon}$ (–0.8 to –0.1‰). Rainwater samples collected in summer from Mt. Kajigamori exhibit high *EFs* of Zn (>10^5).

Dong *et al.* (2017) and Ochoa-Gonzalez *et al.* (2016) investigated Cu and Zn in atmospheric particles and traffic emission sources, and suggested traffic emission as one of the main sources of Cu and Zn in the atmospheric particles. Dong *et al.* (2017) used Sb as an anthropogenic tracer in combination with $\delta^{65}Cu_{NIST976}$ to distinguish the sources of Cu in atmospheric particles. In Fig. 7a,

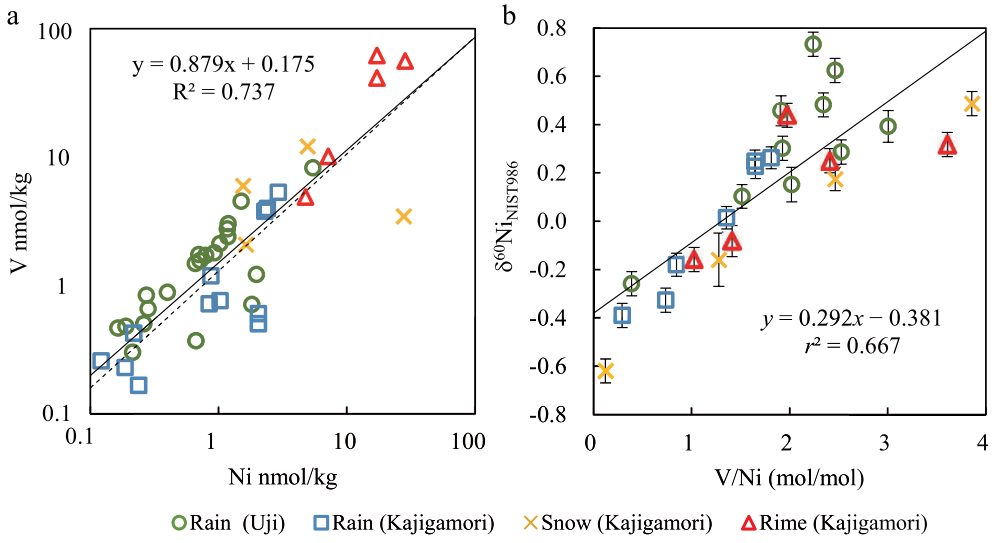

Fig. 8. Vanadium concentrations plotted against Ni concentrations in rainwater, snow, and rime (a). Error bars indicate 2-standard errors of δ values in MC-ICP-MS measurements. The solid line represents the linear regression curve. The dashed line represents the V/Ni ratio in crude oil (Barwise, 1990). $\delta^{60}Ni_{NIST986}$ plotted against V/Ni ratios in rainwater, snow, and rime (b). The solid line represents the linear regression curve.

$\delta^{65}Cu_{NIST976}$ values are plotted against Sb/Cu ratios in our rain, snow, and rime samples. Most of them are plotted in the range of road dust as reported in the previous study (Dong *et al.*, 2017). Therefore, road dust is a dominant source of Cu in rain, snow, and rime collected in Kajigamori and Uji. The high δ^{65}Cu and low Sb/Cu in some samples may be attributed to emission from fossil fuel combustion (Dong *et al.*, 2017; Ochoa-Gonzalez *et al.*, 2016). The high Sb/Cu ratio (>0.4‰) in some samples from Kajigamori is possibly because of the higher solubility of Sb than Cu in fine atmospheric particles (Sarti *et al.*, 2015). In Fig. 7b, $\delta^{66}Zn_{JMC\text{-}Lyon}$ values are plotted against Cu/Zn ratios in the rain, snow, and rime samples. Some of the rain samples obtained from Uji are placed in the range of road dust (Dong *et al.*, 2017). Low $\delta^{66}Zn_{JMC\text{-}Lyon}$ (<0.2‰) values are observed in several rain samples obtained from Uji. The light Zn is likely emitted via high temperature processes in industries, such as smelters and fired power plants, during which light Zn isotopes are preferentially vaporized and emitted into the atmosphere (Mattielli *et al.*, 2009; Ochoa-Gonzalez and Weiss, 2015). Most samples obtained from Kajigamori have lower Cu/Zn ratios than those of the road dust. This suggests an additional source of Zn. The most likely source of Zn would be biomass combustion. The fly ashes from biomass combustion have high Zn content: 9–590 times higher than Cu content (Kovacs *et al.*, 2016; Susaya *et al.*, 2010). Biomass combustion is one of the major sources of anthropogenic aerosols in the Asian continent (Li *et al.*, 2017). Since Mt. Kajigamori is placed at a remote mountain area with a high-altitude of 1400 m, samples collected there are strongly affected by atmospheric particles over long-range transported from the Asian continent (Imai *et al.*, 2017).

Nickel isotopes in aerosols have been reported only for those collected from an island in the South China Sea where the source of Ni is expected to be crude oil combustion, based on the correlation between Ni and V concentrations (Takano *et al.*, 2020). Similar correlation is observed in the rain, snow, and rime samples (Fig. 8a), with a similar slope as that observed in crude oil (Barwise, 1990). Therefore, the dominant source of Ni in these samples is emission from crude oil combustion. $\delta^{60}Ni_{NIST986}$ and V/Ni are found to be correlated (Fig. 8b), which suggests two significant sources of Ni. $\delta^{60}Ni_{NIST986}$ in crude oil from Venezuela and Brazil is reported to be +0.42 to +0.75‰ (Ventura *et al.*, 2015). Therefore, an endmember with high $\delta^{60}Ni_{NIST986}$ would be from the emission of crude oil combustion. Another endmember with low $\delta^{60}Ni_{NIST986}$ cannot be identified in this study, and further study is required.

The Kakita River spring originates from rainwater precipitated on Mt. Fuji, which comes out through basaltic lava layers after ~15 years (Tuchi, 2017). Isotope ratios of Ni, Cu, and Zn in basalts are 0.08 ± 0.19‰ for $\delta^{60}Ni_{NIST986}$ (Cameron *et al.*, 2009; Gueguen *et al.*, 2013), 0.06 ± 0.10‰ for $\delta^{65}Cu_{NIST976}$ (Savage *et al.*, 2015), and 0.30 ± 0.09‰ for $\delta^{66}Zn_{JMC\text{-}Lyon}$ (Liu *et al.*, 2016). These δ values are similar with those of the spring water, implying that Ni, Cu, and Zn in the spring water are prob-

ably supplied from the basaltic lava via water-rock interaction. However, this cannot be firmly concluded due to the small number of samples.

Isotope ratios of Ni, Cu, and Zn in our river water samples are within the range of those reported for rivers worldwide (Fig. 5). $\delta^{60}Ni_{NIST986}$ and $\delta^{65}Cu_{NIST976}$ in the river water are 0.72–1.24‰ and 0.50–0.87‰, respectively. These are significantly heavier than δ values in water sources, such as rain and spring water (Fig. 5). Heavy isotope ratios of dissolved Cu in river water are attributable to the removal of light Cu by adsorption on riverine particles (Vance *et al*., 2008) or oxic soil (Vance *et al*., 2016). For Ni, similar processes would explain heavy isotope ratios in the river water, although isotope ratios of particulate Ni have not yet been determined. $\delta^{66}Zn_{JMC\text{-}Lyon}$ in river water is 0.16–0.38‰, and similar to that of rainwater and spring water (Fig. 5). Unlike Cu, isotope ratios of dissolved and particulate Zn in river water are comparable (Guinoiseau *et al*., 2018), and Zn isotopes are less fractionated in soil environment (Vance *et al*., 2016). Therefore, isotope ratios in dissolved Zn in river water would be comparable to those of rainwater or spring water.

Conclusions

We have presented a novel method for the isotopic analyses of Ni, Cu, and Zn in freshwater samples. This method effectively separates Ni, Cu, and Zn via chelate extraction using a NH_4F solution and anion exchange in CH_3COOH-HCl media. Coexisting elements are low enough in concentrations not to cause detectable interferences in isotopic measurements of Ni, Cu, and Zn. Precision and accuracy have been evaluated via repeat analyses of river water and rainwater. The precision of isotopic analyses for Ni, Cu, and Zn is <0.05‰, which is enough to reveal isotopic variations of Ni, Cu, and Zn in freshwater. Using this method, we have analyzed rain, snow, rime, river water, and spring water in Japan to identify sources of Ni, Cu, and Zn. The $\delta^{65}Cu_{NIST976}$ values and Sb/Cu ratios suggest that road dust is the main source of Cu in most rain, snow, and rime samples collected from Uji and Kajigamori, and that some of the Cu may originate from fossil fuel combustion. Zinc in the rain, snow, and rime samples can be partially attributable to Zn in road dust. $\delta^{66}Zn_{JMC\text{-}Lyon}$ values in the Uji rain samples are lighter than that in the road dust. This light Zn would be emitted via high temperature processes in industrial activities. $\delta^{60}Ni_{NIST986}$ values are correlated with V/Ni ratios in the rain, snow, and rime samples, suggesting heavy oil combustion as their main source. Furthermore, we have analyzed water samples from two rivers and the Kakita River spring in Japan. Nickel and Cu isotope ratios in the river water samples are significantly higher than those in rain, snow and rime samples, while Zn isotope ratios are similar. This is attributed to isotopic fractionation of Ni and Cu between particulate-dissolved phases in river water or soil.

Acknowledgments—We are grateful to Assoc. Prof. Rumi Sohrin for her aid in sample collection from the Kakita River spring. We would also like to thank Prof. Yoshio Takahashi for providing the Taklamakan sand. This study was supported by the Joint Research Grant for Environmental Isotope Study from the Research Institute for Humanity and Nature, the Mitsumasa Ito Memorial Research Grant from the Research Institute for Oceanochemistry Foundation (R2-R2), and JSPS KAKENHI Grants (18K14250, 19H01148 and 20K19957).

References

Archer, C. and Vance, D. (2004) Mass discrimination correction in multiple-collector plasma source mass spectrometry: An example using Cu and Zn isotopes. *J. Anal. At. Spectrom*. **19**, 656–665.

Archer, C., Andersen, M. B., Cloquet, C., Conway, T. M., Dong, S., Ellwood, M., Moore, R., Nelson, J., Rehkamper, M., Rouxel, O., Samanta, M., Shin, K.-C., Sohrin, Y., Takano, S. and Wasylenki, L. (2017) Inter-calibration of a proposed new primary reference standard AA-ETH Zn for zinc isotopic analysis. *J. Anal. At. Spectrom*. **32**, 415–419.

Barwise, A. J. G. (1990) Role of nickel and vanadium in petroleum classification. *Energy & Fuels* **4**, 647–652.

Bigalke, M., Weyer, S., Kobza, J. and Wilcke, W. (2010) Stable Cu and Zn isotope ratios as tracers of sources and transport of Cu and Zn in contaminated soil. *Geochim. Cosmochim. Acta* **74**, 6801–6813.

Borrok, D. M., Wanty, R. B., Ridley, W. I., Wolf, R., Lamothe, P. J. and Adams, M. (2007) Separation of copper, iron, and zinc from complex aqueous solutions for isotopic measurement. *Chem. Geol*. **242**, 400–414.

Cameron, V. and Vance, D. (2014) Heavy nickel isotope compositions in rivers and the oceans. *Geochim. Cosmochim. Acta* **128**, 195–211.

Cameron, V., Vance, D., Archer, C. and House, C. H. (2009) A biomarker based on the stable isotopes of nickel. *Proc. Natl. Acad. Sci*. **106**, 10944–10948.

Chang, Q., Mishima, T., Yabuki, S., Takahashi, Y. and Shimizu, H. (2000) Sr and Nd isotope ratios and REE abundances of moraines in the mountain areas surrounding the Taklimakan Desert, NW China. *Geochem. J*. **34**, 407–427.

Chen, J., Gaillardet, J. and Louvat, P. (2008) Zinc isotopes in the Seine River waters, France: A probe of anthropogenic contamination. *Environ. Sci. Technol*. **42**, 6494–6501.

Chester, R. and Jickells, T. (2012) *Marine Geochemistry*. Willey-Blackwell.

Cong, Z., Kang, S., Zhang, Y. and Li, X. (2010) Atmospheric wet deposition of trace elements to central Tibetan Plateau. *Appl. Geochem*. **25**, 1415–1421.

Conway, T. M. and John, S. G. (2014) Quantification of dissolved iron sources to the North Atlantic Ocean. *Nature* **511**, 212–215.

Dong, S., Weiss, D. J., Strekopytov, S., Kreissig, K., Sun, Y., Baker, A. R. and Formenti, P. (2013) Stable isotope ratio measurements of Cu and Zn in mineral dust (bulk and size fractions) from the Taklimakan Desert and the Sahel and in aerosols from the eastern tropical North Atlantic Ocean. *Talanta* **114**, 103–109.

Dong, S., Ochoa Gonzalez, R., Harrison, R. M., Green, D., North, R., Fowler, G. and Weiss, D. (2017) Isotopic signatures suggest important contributions from recycled gasoline, road dust and non-exhaust traffic sources for copper, zinc and lead in PM10 in London, United Kingdom. *Atmos. Environ*. **165**, 88–98.

Gueguen, B., Rouxel, O., Ponzevera, E., Bekker, A. and Fouquet, Y. (2013) Nickel isotope variations in terrestrial silicate rocks and geological reference materials measured by MC-ICP-MS. *Geostand. Geoanalytical Res*. **37**, 297–317.

Guinoiseau, D., Bouchez, J., Gélabert, A., Louvat, P., Moreira-Turcq, P., Filizola, N. and Benedetti, M. F. (2018) Fate of particulate copper and zinc isotopes at the Solimões-Negro river confluence, Amazon Basin, *Brazil. Chem. Geol*. **489**, 1–15.

Homoky, W. B., John, S. G., Conway, T. M. and Mills, R. A. (2013) Distinct iron isotopic signatures and supply from marine sediment dissolution. *Nat Commun*. **4**.

Hou, H., Takamatsu, T., Koshikawa, M. K. and Hosomi, M. (2005) Trace metals in bulk precipitation and throughfall in a suburban area of Japan. *Atmos. Environ*. **39**, 3583–3595.

Hu, G. P. and Balasubramanian, R. (2003) Wet deposition of trace metals in Singapore. *Water, Air, Soil Pollut*. **144**, 285–300.

Imai, S., Yamamoto, Y., Sanagawa, Y., Kurumi, Y., Kurotani, I., Nishimoto, J. and Kikuchi, Y. (2017) Long-range transport mechanism of cadmium, lead, and nonseasalt-sulfate ion in fresh rime and fresh snow collected on the summit of Mt. Kajigamori, Kochi Prefecture, Japan during the 2008–2014 winter season. *Bunseki Kagaku* **66**, 95–113.

John, S. G. and Conway, T. M. (2014) A role for scavenging in the marine biogeochemical cycling of zinc and zinc isotopes. *Earth. Planet. Sci. Lett*. **394**, 159–167.

Kim, J.-E., Han, Y.-J., Kim, P.-R. and Holsen, T. M. (2012) Factors influencing atmospheric wet deposition of trace elements in rural Korea. *Atmos. Res*. **116**, 185–194.

Kovacs, H., Szemmelveisz, K. and Koós, T. (2016) Theoretical and experimental metals flow calculations during biomass combustion. *Fuel* **185**, 524–531.

Li, Q., Jiang, J., Wang, S., Rumchev, K., Mead-Hunter, R., Morawska, L. and Hao, J. (2017) Impacts of household coal and biomass combustion on indoor and ambient air quality in China: Current status and implication. *Sci. Total Environ*. **576**, 347–361.

Little, S. H., Vance, D., Walker-Brown, C. and Landing, W. M. (2014) The oceanic mass balance of copper and zinc isotopes, investigated by analysis of their inputs, and outputs to ferromanganese oxide sediments. *Geochim. Cosmochim. Acta* **125**, 673–693.

Liu, S.-A., Wang, Z.-Z., Li, S.-G., Huang, J. and Yang, W. (2016) Zinc isotope evidence for a large-scale carbonated mantle beneath eastern China. *Earth. Planet. Sci. Lett*. **444**, 169–178.

Maréchal, C. N., Télouk, P. and Albarède, F. (1999) Precise analysis of copper and zinc isotopic compositions by plasma-source mass spectrometry. *Chem. Geol*. **156**, 251–273.

Mattielli, N., Petit, J. C. J., Deboudt, K., Flament, P., Perdrix, E., Taillez, A., Rimetz-Planchon, J. and Weis, D. (2009) Zn isotope study of atmospheric emissions and dry depositions within a 5 km radius of a Pb-Zn refinery. *Atmos. Environ*. **43**, 1265–1272.

Morel, F. M. M. and Price, N. M. (2003) The biogeochemical cycles of trace metals in the oceans. *Science* **300**, 944–947.

Ochoa-Gonzalez, R. and Weiss, D. (2015) Zinc isotope variability in three coal-fired power plants: A predictive model for determining isotopic fractionation during combustion. *Environ. Sci. Technol*. **49**, 12560–12567.

Ochoa-Gonzalez, R., Strekopytov, S., Amato, F., Querol, X., Reche, C. and Weiss, D. (2016) New insights from zinc and copper isotopic compositions into the sources of atmospheric particulate matter from two major European cities. *Environ. Sci. Technol*. **50**, 9816–9824.

Pan, X., Uno, I., Hara, Y., Osada, K., Yamamoto, S., Wang, Z., Sugimoto, N., Kobayashi, H. and Wang, Z. (2016) Polarization properties of aerosol particles over western Japan: classification, seasonal variation, and implications for air quality. *Atmos. Chem. Phys*. **16**, 9863–9873.

Ratié, G., Quantin, C., Jouvin, D., Calmels, D., Ettler, V., Sivry, Y., Vieira, L. C., Ponzevera, E. and Garnier, J. (2016) Nickel isotope fractionation during laterite Ni ore smelting and refining: Implications for tracing the sources of Ni in smelter-affected soils. *Appl. Geochem*. **64**, 136–145.

Sakata, M. and Asakura, K. (2009) Factors contributing to seasonal variations in wet deposition fluxes of trace elements at sites along Japan Sea coast. *Atmos. Environ*. **43**, 3867–3875.

Sarti, E., Pasti, L., Rossi, M., Ascanelli, M., Pagnoni, A., Trombini, M. and Remelli, M. (2015) The composition of PM1 and PM2.5 samples, metals and their water soluble fractions in the Bologna area (Italy). *Atmos. Pollut. Res*. **6**, 708–718.

Savage, P. S., Moynier, F., Chen, H., Shofner, G., Siebert, J., Badro, J. and Puchtel, I. S. (2015) Copper isotope evidence for large-scale sulphide fractionation during Earth's differentiation. *Geochem. Perspect. Lett*. **1**, 53–64.

Sharrock, P. and Melník, M. (1985) Copper (II) acetates: from dimer to monomer. *Can. J. Chem*. **63**, 52–56.

Siebert, C., Nägler, T. F. and Kramers, J. D. (2001) Determination of molybdenum isotope fractionation by double-spike multicollector inductively coupled plasma mass spectrometry. *Geochem. Geophys. Geosyst*. **2**.

Souto-Oliveira, C. E., Babinski, M., Araújo, D. F. and Andrade, M. F. (2018) Multi-isotopic fingerprints (Pb, Zn, Cu) applied for urban aerosol source apportionment and discrimination. *Sci. Total Environ*. **626**, 1350–1366.

Souto-Oliveira, C. E., Babinski, M., Araújo, D. F., Weiss, D. J. and Ruiz, I. R. (2019) Multi-isotope approach of Pb, Cu and Zn in urban aerosols and anthropogenic sources improves tracing of the atmospheric pollutant sources in megacities. *Atmos. Environ*. **198**, 427–437.

Stefania, G., Stoica, C., Vasile, G., Nita-Lazar, M., Elena, S. and Lucaciu, I. (2017) Metals Toxic Effects in Aquatic Ecosystems: Modulators of Water Quality.

Susaya, J., Kim, K.-H., Ahn, J.-W., Jung, M.-C. and Kang, C.-H. (2010) BBQ charcoal combustion as an important source of trace metal exposure to humans. *J. Hazard. Mater*. **176**, 932–937.

Takano, S., Tanimizu, M., Hirata, T. and Sohrin, Y. (2013) Determination of isotopic composition of dissolved copper in seawater by multi-collector inductively coupled plasma mass spectrometry after pre-concentration using an ethylenediaminetriacetic acid chelating resin. *Anal. Chim. Acta* **784**, 33–41.

Takano, S., Tanimizu, M., Hirata, T., Shin, K.-C., Fukami, Y., Suzuki, K. and Sohrin, Y. (2017) A simple and rapid method for isotopic analysis of nickel, copper, and zinc in seawater using chelating extraction and anion exchange. *Anal. Chim. Acta* **967**, 1–11.

Takano, S., Liao, W.-H., Tian, H.-A., Huang, K.-F., Ho, T.-Y. and Sohrin, Y. (2020) Sources of particulate Ni and Cu in the water column of the northern South China Sea: Evidence from elemental and isotope ratios in aerosols and sinking particles. *Mar. Chem*. **219**, 103751.

Takeda, K., Marumoto, K., Minamikawa, T., Sakugawa, H. and Fujiwara, K. (2000) Three-year determination of trace metals and the lead isotope ratio in rain and snow depositions collected in Higashi-Hiroshima, Japan. *Atmos. Environ*. **34**, 4525–4535.

Tanner, P. A. and Wong, A. Y. S. (2000) Soluble trace metals and major ionic species in the bulk deposition and atmosphere of Hong Kong. *Water, Air, Soil Pollut*. **122**, 261–279.

Tuchi, R. (2017) Geology and groundwater of Mt. Fuji, Japan. *J. Geography*. **126**, 33–42.

Vance, D., Archer, C., Bermin, J., Perkins, J., Statham, P. J., Lohan, M. C., Ellwood, M. J. and Mills, R. A. (2008) The copper isotope geochemistry of rivers and the oceans. *Earth. Planet. Sci. Lett*. **274**, 204–213.

Vance, D., Matthews, A., Keech, A., Archer, C., Hudson, G., Pett-Ridge, J. and Chadwick, O. A. (2016) The behaviour of Cu and Zn isotopes during soil development: Controls on the dissolved load of rivers. *Chem. Geol*. **445**, 36–53.

Ventura, G. T., Gall, L., Siebert, C., Prytulak, J., Szatmari, P., Hürlimann, M. and Halliday, A. N. (2015) The stable isotope composition of vanadium, nickel, and molybdenum in crude oils. *Appl. Geochem*. **59**, 104–117.

Yamakawa, A., Yamashita, K., Makishima, A. and Nakamura, E. (2009) Chemical separation and mass spectrometry of Cr, Fe, Ni, Zn, and Cu in terrestrial and extraterrestrial materials using thermal ionization mass spectrometry. *Anal. Chem*. **81**, 9787–9794.

Yamamoto, Y., Sanagawa, Y., Kurumi, Y., Saito, A., Nishimoto, J., Kikuchi, Y. and Imai, S. (2019) Nonanthropogenic levels of cadmium, lead, and non seasalt-sulfate in rain and snow water collected in remote areas in Japan. *Bunseki Kagaku* **68**, 51–64.

Yang, S.-C., Welter, L., Kolatkar, A., Nieva, J., Waitman, K. R., Huang, K.-F., Liao, W.-H., Takano, S., Berelson, W. M., West, A. J., Kuhn, P. and John, S. G. (2019) A new anion exchange purification method for Cu stable isotopes in blood samples. *Anal. Bioanal. Chem*. **411**, 765–776.

Ye, L., Huang, M., Zhong, B., Wang, X., Tu, Q., Sun, H., Wang, C., Wu, L. and Chang, M. (2018) Wet and dry deposition fluxes of heavy metals in Pearl River Delta Region (China): Characteristics, ecological risk assessment, and source apportionment. *J. Environ. Sci*. **70**, 106–123.

Zheng, M., Guo, Z., Fang, M., Rahn, K. A. and Kester, D. R. (2005) Dry and wet deposition of elements in Hong Kong. *Mar. Chem*. **97**, 124–139.

Zhu, Z. Y., Jiang, S. Y., Yang, T. and Wei, H. Z. (2015) Improvements in Cu-Zn isotope analysis with MC-ICP-MS: A revisit of chemical purification, mass spectrometry measurement and mechanism of Cu/Zn mass bias decoupling effect. *Int. J. Mass Spectrom*. **393**, 34–40.

Supplementary Materials

URL (http://www.terrapub.co.jp/journals/GJ/archives/data/55/MS627.pdf)
Figures S1 to S4
Tables S1 to S12